Journal of Renewable Materials

Tech Science Press

DOI: 10.32604/jrm.2023.027372

ARTICLE

Novel Pectin/Chia-Mucilage Membranes: Human Serum Albumin Adsorption, Biocompatibility, and Physical-Chemical Properties

S. E. Burruel-Ibarra[1], R. A. Esquer-Osuna[2], R. G. Valdez-Melchor[2], D. A. Cuevas-Acuña[2], L. Quihui-Cota[3], J. Juárez[4], J. C. Campos-García[2], E. Valbuena-Gregorio[2] and M. A. López-Mata[2,*]

[1]Departamento de Investigación en Polímeros y Materiales, Universidad de Sonora, Hermosillo, Sonora, México

[2]Departamento de Ciencias de la Salud, Campus Cajeme, Universidad de Sonora, Cd. Obregón, Sonora, México

[3]Departamento de Nutrición Pública y Salud, Coordinación de Nutrición, Centro de Investigación en Alimentación y Desarrollo, A. C., Hermosillo, Sonora, México

[4]Departamento de Física, Universidad de Sonora, Hermosillo, Sonora, México

[*]Corresponding Author: M. A. López-Mata. Email: marco.lopezmata@unison.mx

Received: 27 October 2022 Accepted: 22 December 2022

ABSTRACT

This study aimed to characterize the physical-chemical and biological properties of pectin (PC)/chia seed mucilage (CM) membranes. PC/CM [100/0 (control), 80/20%, 60/40%, and 40/60% w/w] membranes were prepared using the casting method. The membranes (PC/CM) were thin, yellow, lightly opaque (≈10%) and capable of blocking light UVB (between 66 at 52%). SEM analysis showed the presence of aggregates in the shape of a sphere (≈13 μm) and ovoid (≈25 μm). The proportion of 80/20 showed an increase in tensile strength (29%) and elastic modulus (19%) when compared to the control. FTIR analysis exhibited intermolecular interactions between PC-PC, PC-CM, and CM-CM in the membranes. The thermal analysis (600°C) showed a slight improvement in the percentage of residual mass-loss of 3.31% (80/20) that control. The 40/60 membrane showed the lowest percentage of hemolysis (2.94%) but limited human albumin adsorption capacity. These results suggested that the blend PC/CM may be considered as a biomaterial for medical applications.

KEYWORDS

Pectin; chia mucilage; membrane; hemolysis; albumin; biomaterial

Nomenclature

PC	Pectin
CM	Chia seed mucilage
TS	Tensile strength
%E	Elongation at break
ME	Tensile modulus of elasticity

1 Introduction

The concern for developing novel biomaterials is increasing due to the residue or impurities detected in synthetic polymers that may affect the tissues preventing adequate cell growth [1]. In addition, synthetic polymer materials are often associated with chronic inflammation, immunological reactions, and toxicity [2]. The replacement of synthetic polymers is difficult because of their better mechanical, thermal stability, and malleable properties than those of biopolymers [3]. However, biopolymers are low-cost, biodegradable, biocompatible, non-toxic, and able to absorb corporal fluids and release bioactive compounds on the target tissues, which are all significant in the development of medical and pharmaceutical applications [4]. The biopolymers used to elaborate biomedical materials come from animals (e.g., keratin, chitosan, collagen and elastin) and plant sources (polysaccharides mainly). That is why the polysaccharides acquired from plants have gained enormous attention and are considered an alternative green for the generational replacement of synthetic materials [5]. The main polysaccharides used in biomaterials preparation for the biomedical field are starch [6], cellulose [7], mucilage [8], and pectin [9]. Pectin (PC) is chemically a linear polymer of *D*-galacturonic acid with α (1–4) linkages sequences [10] that may also contain different monosaccharides domains (around 17). PC has been proposed as a biomaterial for developing drug-controlled delivery systems [11], wound dressing [12], wall material for bioactive microencapsulation [13], and reinforcement for other materials [14].

On the other hand, *Salvia hispanica* L. is a plant widely used as a source of food, medicine, and oil since pre-Columbian Mesoamerica [15]. This plant gives seeds that in water can release a transparent mucilage with a high capacity of water retention (27 times its weight) similar to guar gum [16], with high viscosity and gelling properties [17]. Based on its functionality, it is hypothesized that the chia-mucilage (CM) in the plant may have essential roles such as cold tolerance, wound healing, water transport, and other functions. This functionality has been associated with their chemical composition based probably on the presence of xylose, glucose, and fundamental units of polysaccharides with a tentative structure of tetrasaccharide with 4-O-methyl α-*D*-glucoronopyranosyl residues on the main chain and ramification of β-xylopyranosyl [18]. An analysis of their microstructure also revealed that these polysaccharides have the property of forming a network structure with open pores and the capacity of water retention [15]. Additionally, the CM is considered nontoxic, biodegradable, widely available in nature, and renewable; and it has been screened in the pharmaceutical and medical industries for different uses such as wall material for encapsulation, drug delivery and wound dressing. CM is a good candidate for the development of wound dressing due to its antioxidant, antimicrobial, anti-inflammatory mucoadhesive and cytocompatibility properties [19,20]. However, some biomaterials of CM used as wound dressing tend to be brittle and show poor mechanical properties [16]. Combinations of CM with other biopolymers matrices such as starch nanocrystals [21], whey protein [22], and cellulose nanofibers [23] have been developed to search for better mechanical and biological properties. Dehghani et al. developed nanofiber mixing CM, polyvinyl alcohol (40:60 proportion) and cardamonmum essential oils (used electrospinning process). These nanofibers showed encapsulation capacity, antibacterial (against Gram positive and negative bacteria) and antioxidant activity [24]. Also, Luo et al. found that gelatin/CM films incorporated with oregano essential oils (using the casting method) showed adequate compatibility and antibacterial activity, however, the increase of CM proportion in films increased their rigidity and reduced their extensibility [25]. Other blends of levan (homopolysaccharide of fructose) and different degrees of CM (obtained to 25, 55 and 80°C) and sorbitol have shown reduced stress at break. Additionally, anti-quorum sensing (*Chromobacterium*

violaceum) properties were attributed to the presence of CM in the films (55°C), but some cracks also have been observed on their surface [26]. Although, CM blends with other biomaterials have shown adequate biological properties to be used as wound dressing [27], mechanical fragility limits their application. While it is true that CM is an important component to be used as biomaterial, interest in developing novel biomaterials based on blends with other biopolymers remains to provide better structural support to MC and maintain its biological properties. That's why it is thought that blends of PC/CM may generate a reinforcement in the biopolymeric network of CM to obtain fewer brittle biomaterials with better mechanical and physical properties. Therefore, this work aimed to characterize the physical-chemical and biological properties of novel membranes based on the blend PC/CM.

2 Materials and Methods

2.1 Materials

Chía seed (*Salvia hispanica* L.) was obtained from a market located in Cd. Obregon, Sonora (Northwest Mexico). The citrus pectin (PC) was provided for Faga Lab® food grade with ≈65% *D*-galacturonic acid (FAVELA PRO, SA DE CV, Sinaloa, Mexico). All reagents used were grade or higher quality.

2.2 Extraction of Chia Mucilage

Firstly, chia seeds were washed with distilled water and left in water [1:30 w/v] for two hours at 50°C and non-stirring. Then, chia seeds-water was collocated in constant stirring for three h and then filtered through nylon mesh to remove seeds. The material filtered was centrifuged at 200 *g* for 15 min to discard seed remains. Finally, CM was taken from the supernatant and divided into aliquots to keep them at −20°C until processing.

2.3 Membrane Preparation

Firstly, a PC solution at 3.0% [w/v] was prepared to elaborate the membranes. Then, blends of PC/CM were prepared as follows: 100/0 (control), 80/20%, 60/40%, and 40/60% [w/w]. These blend membrane solutions were placed in a Petri dish (triplicate) and dried in an oven (Binder-FD53) at 40°C for 48 h. The formed membrane was placed in a desiccator with silica gel at 25°C until analysis.

2.4 Thickness Measurement

A micrometer (Mitutoyo, Japan, precision = 0.001 in) was used to measure the membranes' thickness. Randomly, six measurements of thickness per membrane were carried out and expressed in mm.

2.5 Optical Properties

Transparency was determined by the method of Han et al. [28]. Firstly, rectangles of membranes of 9 × 45 mm were cut and placed inside the spectrophotometer cell (Jenway 7305, UK). Otherwise, the transmittance was calculated at 600 nm, and the transparency of the membranes was calculated using the Eq. (1).

$$Transparency = \log(T600/t) \tag{1}$$

T600 corresponds to transmittance at 600 nm; t represents the membrane thickness (mm).

In addition, color and opacity were measured using an X-rite SP-64 spectrophotometer, calibrated with white and black standard plates. The membranes were randomly chosen for analysis, and five measurements

were performed. All results were based on the CIE model (L^* a^* y b^*). Each membrane's opacity (%) was analyzed over white and black standards, and the opacity was calculated using the Hunterlab color scale [29].

2.6 ATR-FTIR Analysis

Firstly, five milligrams of each membrane (by triplicate) were scanned (2 cm^{-1} of resolution) and monitored the wavenumber region of 400–4000 cm^{-1} with an ATR-FTIR Perkin-Elmer 1600 spectrophotometer in transmittance mode. This study evaluated the intermolecular interaction sites of the membrane PC-PC, PC-CM components, and CM-CM biopolymers.

2.7 Microstructure Study

SEM studied the microstructure and interaction of the PC/CM membranes. Samples were carefully cut, then coated with gold-palladium to impart conductive properties and viewed on a scanning Electron Microscopy [JEOL JSM-5410LV, Japan] with an INCA system and Energy Dispersive X-Ray (EDS) detector operated at 20 kV [30].

2.8 Mechanical Properties

The tensile strength (TS), %elongation (%E), and elastic modulus (EM) were determined using the standard method ASTM-D882-12. PC/CM membranes. Initially, membranes in rectangles of 6.0 × 1.0 cm were cut and conditioned at 52% relative humidity (RH, used NaBr) for 24 h. Then, the membranes were analyzed utilizing a texture meter TAXT-Plus (UK) under 30 kg load, an initial gauge of 4 cm length, and stretched using a crosshead speed of 20 mm•min^{-1}. TS (MPa), %E (%), and EM (MPa) were calculated using Exponent Lite Software. Each membrane was analyzed five times.

2.9 Thermal Analysis

The thermal stability of the compounds from PC/CM membranes was determined by a Perkin-Elmer Thermogravimetric Analyzer model Pyris 1. Samples of the membrane (2.4 mg) were weighed and subjected to healing from 30 to 800°C (using a healing rate of 10 °C•min^{-1}) under a nitrogen atmosphere. Thermogravimetric curves of the mass loss rate were obtained.

2.10 Human Serum Albumin Adsorption

Firstly, a human lyophilized serum obtained from SPINREACT company (spintrol H: calibrator of multi-components for clinical chemistry assays—SPINREACT®, Girona, Spain) was reconstituted using 5.0 mL distilled water and mixed thoroughly to prevent foam forming. This human serum contained the albumin concentration of well-known reference to be measured by the bromcresol green colorimetric method. After, the mix was used to have an approximation of the capacity of each membrane (6 mm-disk) to catch serum volume, where both maximal and minimal catchment were observed for the control (45 µL) and 40/60 (40 µL), respectively (Fig. 1), to obtain a margin of sufficient volume of sample (adjustment 80 µL) to be used in the albumin adsorption test.

Eighty microliters of serum were added to an Eppendorf tube that contained a 6 mm-disk of the membrane. The tubes were incubated at 37°C for two h (Binder incubator, Germany); and later, they were centrifuged at 11,000 *g* (SIGMA-1-15P, Germany) for 10 min. Twenty microliters of supernatant were mixed in 2.0 mL bromcresol green [0.12 mmol/L, and pH 4.2] (SPINREACT® kit), and the mix was incubated at room temperature for 10 min. Subsequently, the absorbance for the mix was determined at 630 nm (Jenway model 7205 spectrophotometer, UK). Finally, results were calculated according to Eq. (2) and expressed as albumin adsorption percentage (%RA).

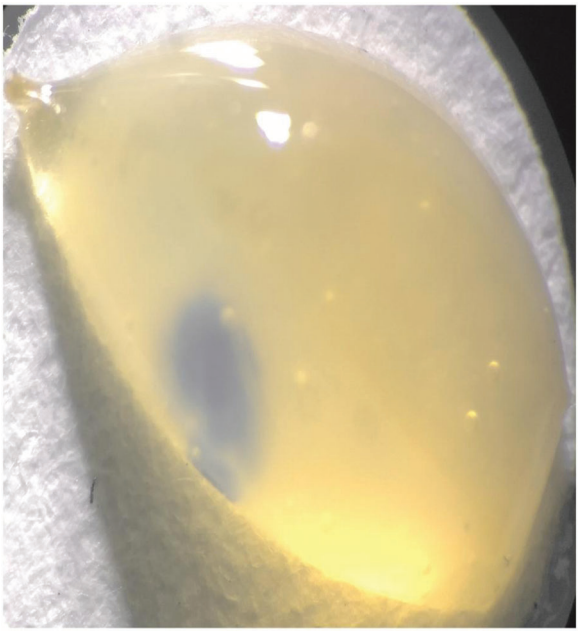

Figure 1: Human serum catchment by the membrane, taking a cocoon form

$$\%RA = \frac{CAC - CAM}{CAC} \times 100 \tag{2}$$

where CAC = Albumin concentration in the no membrane calibrator; CAM = Albumin concentration with added membrane.

2.11 Erythrocyte Biocompatibility Test

Firstly, the erythrocytes were washed three times in saline solution (NaCl, 0.9% w/v) to remove components from the plasma. Afterward, an erythrocyte suspension (5.0% v/v) was prepared using a saline solution. Eppendorf tubes with a membrane of 6 mm disk were placed on the top, and 200 µL erythrocyte suspension was added and incubated at 37°C for two h (BINDER incubator, Germany). Then, 200 µL of saline solution was added and centrifuged at 2700 × *g* for 10 min. Later, 200 µL supernatant was dissolved in 2.0 mL distilled water and read at 540 nm. One sample of 100% hemolysis–erythrocyte and water–was used as a reference to calculate the hemolysis percentage [hemolysis (%)] using Eq. (3):

$$Hemolysis\ (\%) = \frac{AHS}{AHC} \times 100 \tag{3}$$

where AHS = Hemolysis absorbance of the sample; AHC = Complete hemolysis absorbance.

2.12 Statistical Analysis

The PC/CM membrane concentrations were assigned as independent variables, and the optical, mechanical, TGA, percentage of hemolysis, and percentage of albumin retention as response variables in the variance analysis. The difference among the means was estimated using the Duncan test ($\alpha = 0.05$). All statistical analyses were carried out using the NCSS software, version 2000.

3 Results and Discussion

3.1 Optical Properties

Transparency partially determines the miscibility or compatibility of biopolymer blends and the stability of microstructure [31]. Additionally, medical devices usually require acceptable transparency to visualize through material [32]. All membranes were transparent (Fig. 2), and although the control had the highest transparency this also had high thickness (Table 1).

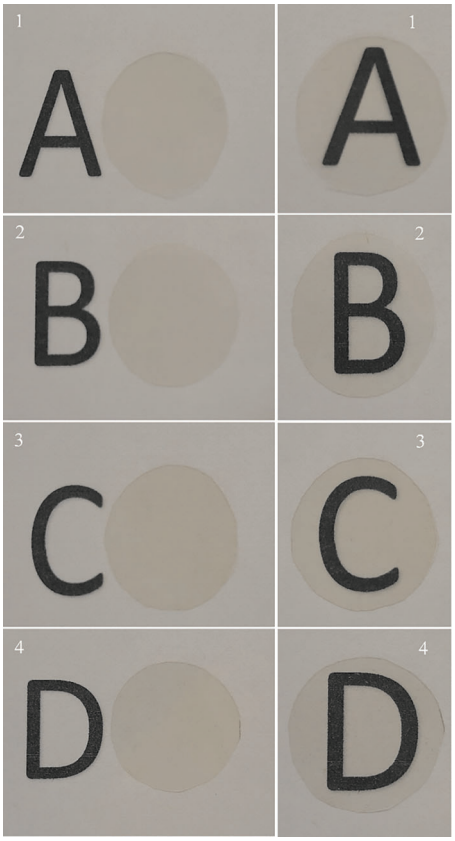

Figure 2: Images of PC/CM membranes: 100/0 (**1**), 80/20 (**2**), 60/40 (**3**) and 40/60 (**4**) on the left (membrane beside the letter) and right (membranes in front of the letter)

Table 1: Color, opacity and transparency of PC/CM membranes

PC/CM (%)	*L**	*a**	*b**	Opacity (%)	Transparence values
100/0	92.3 ± 0.02^{a}	-1.71 ± 0.06^{a}	7.89 ± 0.03^{a}	10.49 ± 0.03^{a}	2.78 ± 0.05^{a}
80/20	92.8 ± 0.10^{a}	-1.50 ± 0.06^{b}	5.67 ± 0.22^{b}	10.20 ± 0.11^{a}	3.01 ± 0.04^{b}
60/40	90.3 ± 0.16^{b}	-1.61 ± 0.05^{c}	12.83 ± 0.35^{c}	10.37 ± 0.35^{a}	3.13 ± 0.05^{c}
40/60	91.3 ± 0.21^{c}	-1.67 ± 0.01^{d}	10.92 ± 0.70^{d}	10.51 ± 0.29^{a}	3.02 ± 0.04^{b}

Note: *Results are expressed in mean ± standard error, and different letters in the same column indicate differences by Duncan test ($p < 0.05$).

Some authors have reported that thickness can act significantly to the detriment of the membrane's transparency [33]. Conversely, the addition of CM resulted in thin membranes and reduced ($p < 0.05$) transparency of the PC/CM membranes in 8.27% (80/20), 12.58% (60/40), and 8.63% (40/60), as

compared to the control. Other prepared membranes with polysaccharides blend (chitosan and guar gum) were lesser transparent (46.96–53.87 values) than our membranes. This was attributed to guar gum and water molecules, which modified the refractive index of chitosan [34]. López-Mata et al. made a blend of *Aloe* gel with egg white (protein animal) to obtain membranes with good transparency values (2.04–2.57), and more transparent than those in this study [35].

Usually, transparency and opacity are considered opposite properties in the optical area. Nevertheless, the measurement of transparency in the membranes is calculated with the transmittance, which depends on color, thickness, and interference fringes (slight) [36]. Otherwise, opacity is calculated using a black and white backing from the reflectance measurements of membranes [37]. Therefore, changes in the transparency values are not necessarily related to a significant change in the opacity (Table 1). The addition of CM in the membranes resulted only in transparency changes but not in opacity. In our study, all the membranes showed low opacity (≈10%), similar to those reported in two CM/whey protein membranes (proportions 1/3 and 1/4) [22], and membranes based on PC/*Aloe*-gel [38].

The ability of a biomaterial to interact with middle-wave ultraviolet radiation (UVB) in the spectral region has been reported as wavelength ranges that may induce skin damage and wound healing delay [39]. Our results suggested that all membranes at 280 nm (Fig. 3), can block UVB light between 52% and 66%, and the CM addition did not necessarily improve this attribute. Similar behavior was also observed at 350 nm. In comparison with other blends of matrices such as chitosan/guar gum (>90%) [34] or PC/*Aloe*-gel (>72%) [38], our PC/CM had the lowest efficiency in blocking UVB.

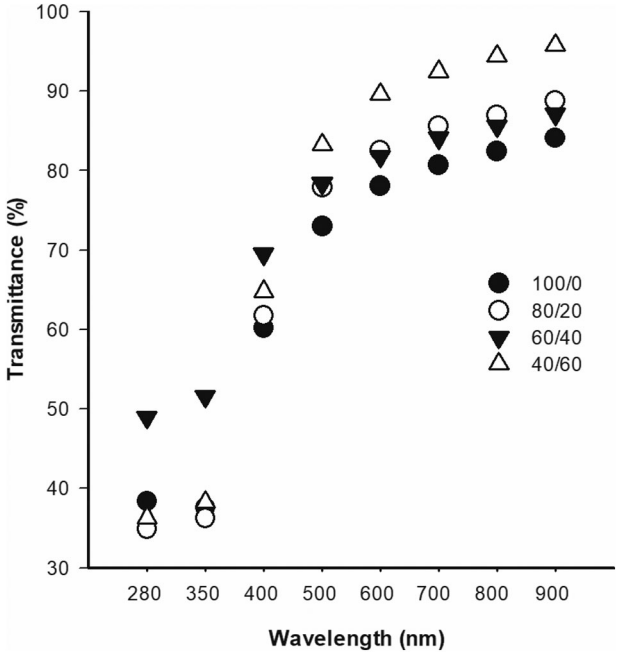

Figure 3: Light transmittance (%) of PC/CM membranes

Color parameters (a^*, b^*, and L^*) of the membranes are also presented in Table 1. The lightness (L^*) in all membranes was good, but the increase in the CM ratio (60/40 and 40/60 membranes) significantly reduced lightness. Similar behavior was observed for the b^* value, where an increase of the CM in the composition of the membrane resulted in increased yellow coloration ($p < 0.05$). These changes may depend on the optical configuration produced by both the molecular organization and the seed compounds contained in the mucilage during the membrane development [16].

3.2 Microstructure

SEM analysis is essential to recognize the microstructure and interaction of the membrane components. Fig. 4 shows the scanning electron micrograph of the membranes obtained. It displays the morphological evolution of the PC membrane across the addition of different proportions of CM. It was observed a homogeneous ribbed surface on the control membrane. Previous studies also reported grooves and rivers marks in protein animal membranes [40] similar to our control. The formation of these channels may be associated with a molecular realignment of the polysaccharides during the water loss. Cokaygil et al. analyzed the microstructural surface of membranes of pectin orange peel and corn starch with layered silicates, and grooves on the membrane surface were associated with fractures [41]. The addition of CM in 80/20 proportion resulted in a homogeneous, smooth, non-porous and non-grooved surface of this membrane. However, a significant increase in the proportion of CM (60/40 and 40/60 membranes) resulted in a sphere (≈13 μm), ovoid (≈25 μm) [shadow black (40/60)], and amorphous aggregates (white). Krystyjan et al. reported that the addition of mucilage in starch/*Plantago psyllium* seed mucilage membrane formed spherical particles similar to those in this study [42], probably associated with microcapsules formation (size 150–200 nm). In addition, the increase of white particles with granular forms may be attributed to a displacement of insoluble material on the surface of PC by an increase of CM amount (high water content) as previously reported [22].

3.3 Mechanical Properties

Table 2 shows the mechanical properties, expressed by tensile strength (TS), elongation at break (%E), and tensile modulus of elasticity (ME) of PC/CM membranes. Good resistance to plastic deformation has been reported for the PC membranes, but limitations such as rigidity and brittleness are present [43]. Our control (only PC) showed similar TS and flexibility as compared with high (TS = 20 MPa, %E = 17) and low (TS = 19 MPa, %E = 17) methyl ester PC membranes, although the elastic modulus was lower in our membranes [44]. This behavior may result from a channel formed on the surface of the control (See SEM analysis), that may affect the membrane lability when subjected to an extension upon tension, causing loss of structural integrity of the membrane [45]. The 80/20 blend showed a significant increase of 29% and 19% in the TS and ME, respectively, compared to the control. This increase in resistance and flexibility may be associated with interactions between PC and CM components. A significant proportion of CM (60/40 and 40/60) in the membrane showed no significant improvement in TS and %E. This may result in the displacement of insoluble material (showed in SEM analysis) affecting the degree of interactions of the membrane components. Initially, the 80/20 membrane was more rigid than the control, while the 60/40 membrane showed the highest flexibility (ME decreased). Significant changes were observed in ME, probably associated with the plasticizer used [46], or changes in the interaction and alignments among the PC chains and CM as recorded previously for fish gelatin/*Aloe* membranes [47].

3.4 ATR-FTIR Analysis

Fig. 5 shows the FTIR analysis spectra of the blends of PEC/CM. This test analyzed the intermolecular interaction between components of the membrane. It was observed that the transmittance bands and peaks at 3287 cm^{-1} (-OH), 2990 (-O-CH_3^-), and 2880 cm^{-1} (-CH_2^-) are specific to PEC. Additionally, the band centered in 1731 and 1620 cm^{-1} is attributed to the stretching vibration of -COO-CH_3 and -COO^-, respectively. The stretching of the C-O-C bond of the pyranose ring was identified in the adsorption peaks located at 1230 and 1015 cm^{-1} [46]. The FTIR spectrums of membrane blends of PEC with CM exhibited changes, particularly in the -OH band when CM increased. These changes indicated intermolecular interaction between PEC-PEC, PEC-CM, and CM-CM biopolymers, mediated by -OH and -COOH groups through the formation and disruption of hydrogen bonds [48]. As the amount of hydrogen bonds was proportional to the intensity of the -OH band, it was suggested that the ratio of hydrogen bonds disrupted in PC-PC is greater than the hydrogen bonds formed in the intermolecular association of

PC-CM, due to the low number of -OH groups in the chia mucilage. On the contrary, the transmittance % intensity for the -OH band decreased at a higher ratio of CM (40/60), because the great ability of CM to adsorb water molecules [21].

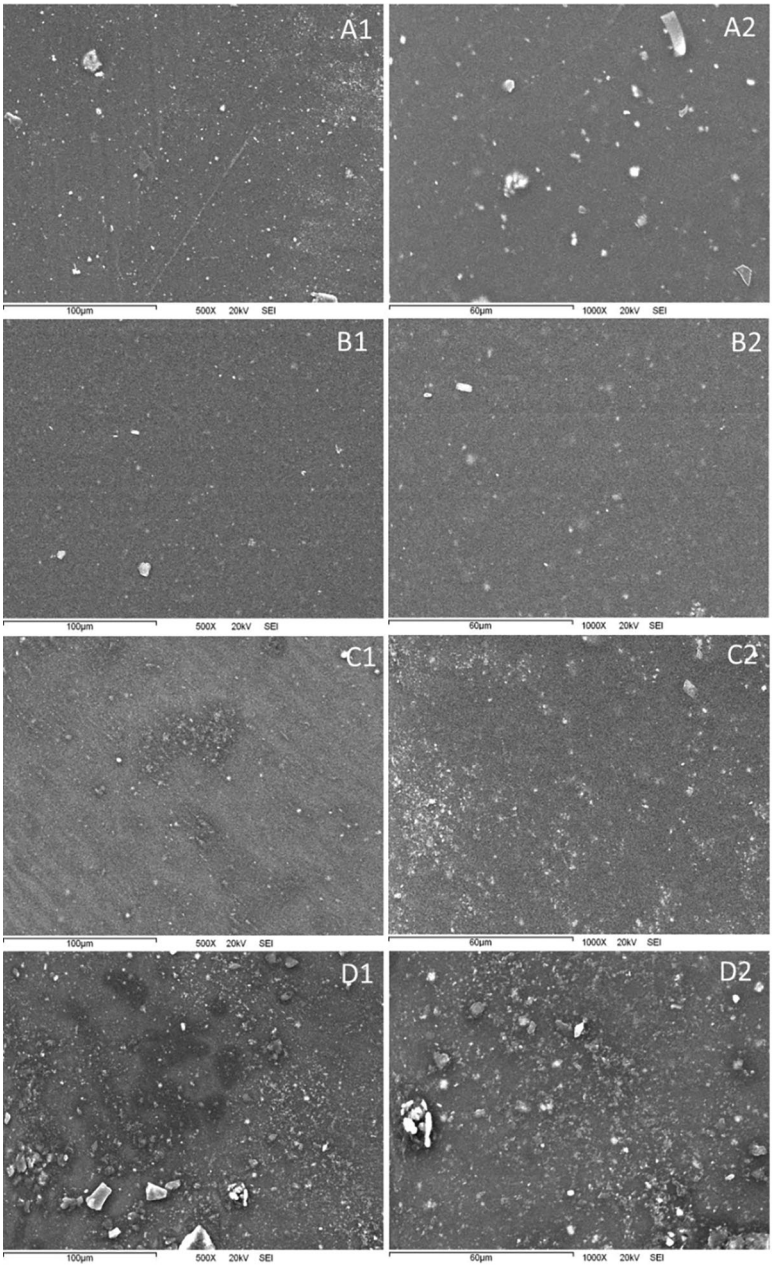

Figure 4: SEM images of the surface PC/CM membranes, where letters and numbers are interpreted as follows: A1 and A2 (100/0), B1 and B2 (80/20), C1 y C2 (60/40), D1 y D2 (40/60)

Table 2: Mechanical properties and thickness of the PC/CM membranes

PC/CM (%w/w) films	TS (MPa)	%E	EM (MPa)	Thickness (mm)
100/0	20.17 ± 1.15[a]	19.45 ± 1.12[a]	352.14 ± 9.66[a]	0.121 ± 0.010[a]
80/20	26.04 ± 0.80[b]	18.18 ± 1.24 [a]	420.55 ± 7.65[b]	0.071 ± 0.005[b]
60/40	21.40 ± 1.12[a]	20.62 ± 0.53 [a]	301.30 ± 8.92[c]	0.075 ± 0.010[b]
40/60	22.69 ± 3.19[a]	19.45 ± 1.12 [a]	372.95 ± 10.20[d]	0.070 ± 0.015[b]

Note: *Results are expressed in mean ± standard error and different letters in the same column, indicate significant differences by Duncan test ($p < 0.05$).

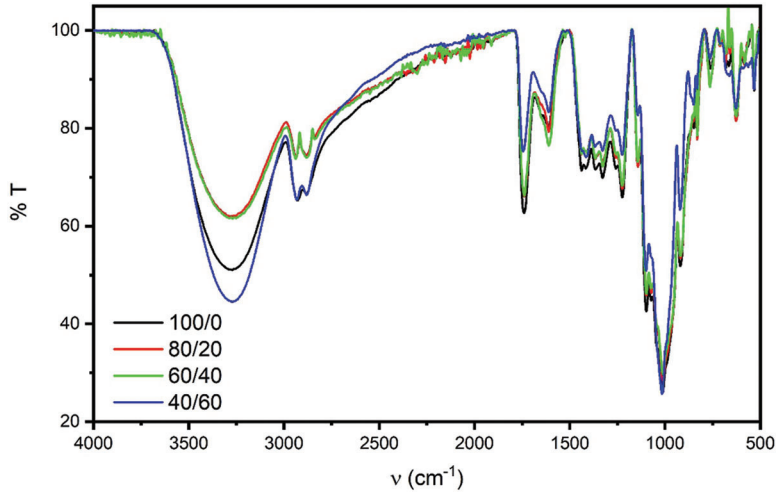

Figure 5: Fourier-transform infrared spectra of PC/CM membranes

3.5 Thermogravimetric Analysis (TGA)

Thermal resistance of the biopolymeric membranes was measured by thermogravimetry characterization. This technique is based on determining a loss or gain mass of the sample concerning temperature and time (controlled temperature increase), indicating the temperature range at which the membrane components start decomposing [49]. Fig. 6 shows the analysis of the TGA thermograms of the membranes.

The control membrane showed a loss weight of 8.29% at 84°C associated with water evaporation. The first loss of weight in all the membranes with CM was 3.37% (80/20), 13.10% (60/40), and 12.05% (40/60) at 89.6°C, 81.3°C, and 82.3°C, respectively. A similar loss weight, around 6.0%–9.0%, was associated with the desorption of loss moisture linked by hydrogen bonds to the polysaccharides of CM, as previously reported [23]. The second thermal event observed at 102°C–199°C corresponds to glycerol degradation used during the membrane development. Similar thermal behavior of the glycerol in the edible membrane of CM has been observed previously [16]. High membranes' losses were observed at around 200°C–280°C (between 43%–50% loss) in the third thermal event, associated with the thermal degradation of polysaccharides in the PC and CM. Giancone et al. and de Campo et al. reported a similar thermal degradation of polysaccharides in PC and CM. Another thermal event showed maximum peaks around 312.7°C, which meant a weight loss from

19% to 28% in the control membrane [4,50]. Other temperature peak events at 600°C may be attributed to the decomposition of structures produced due to crosslinking reactions during the heating procedure [51].

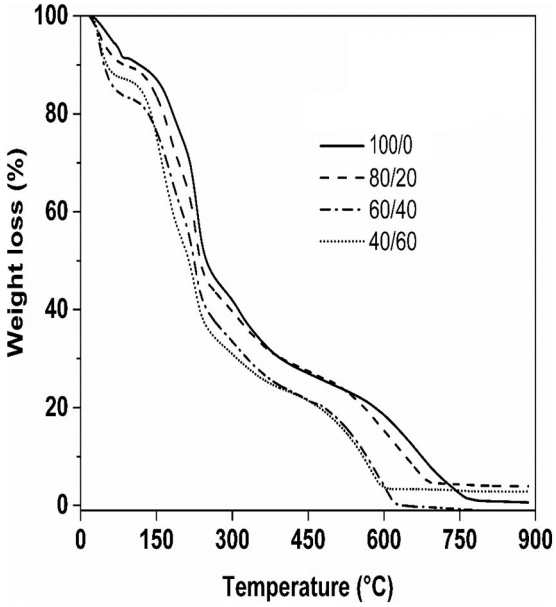

Figure 6: TGA curves of PC/CM membranes

The low residual mass-loss for 80/20 (4.58%) and 40/60 (2.52%) membranes as compared with control (1.27%), revealed that incorporation of CM in the described proportions, resulted in a slight improvement in thermal stability. Krystyjan et al. found that mucilage addition may fill areas among starch molecules in the microcapsule inside starch/*Plantago psyllium* mucilage seed membranes, probably resulting in more thermally stable membranes [42]. In previous CM nanocomposite membranes with starch nanocrystals, a similar behavior has also been observed [23]. This study also revealed the presence of CM microencapsulated inside the PC matrix during SEM analysis.

3.6 Human Serum Albumin Adsorption

When a wound dressing is placed on damaged tissue, interaction with blood and serum proteins occurs, and they may be adsorbed on the biomaterial surface. The adsorbed serum proteins may change the initial activity of the biomaterial surface probably modulating the direction of the immune response of the biomaterial [52]. Fig. 7 shows the percentage of human albumin retention from the serum of the tested membranes.

The control (11.4%) and the 80/20 (6.5%) membranes showed albumin retention capacity, being the control that showed ($p < 0.05$) the highest retention.

Both 60/40 and 40/60 membranes did not show albumin retention capacity, indicating that the PC amount mediates the albumin adsorption in the membrane, while the CM had reduced the albumin adsorption. Cacidedo et al. [53] found 10 times higher the incorporation of human serum albumin in hybrid bacterial cellulose-pectin films than in the control (bacterial cellulose) using a fluorescence

technique. The PC chemical structure has an important influence on the albumin adsorption [53]. The presence of free carboxyl groups (negatively charge) in the PC may explain the albumin adsorption (positively charge in serum) in the membranes [54]. Other studies based on the bovine serum albumin adsorption capacity of PC gel bead, reported that this property may also be attributed to Van der Waals interactions, hydrogen bonding and hydrophobic interactions of the chemical structure of the albumin and PC [55]. Visalakshan et al. also reported that albumin had a high affinity with carboxyl functional groups from a variety of biomaterials. They observed that the bound surface with albumin did not trigger an immune response [56], which is particularly important in reducing the probability of rejection of biomaterials in the tissues [57]. The biomaterial-albumin bound may also be advantageous as wound dressing because the albumin on the biomaterial surface can influence the reduction of proinflammatory cytokines [58]. On the other hand, it is relevant to mention that the adsorption capacity of other plasmatic proteins, probably occurred in the membranes, although they were not quantified in this study.

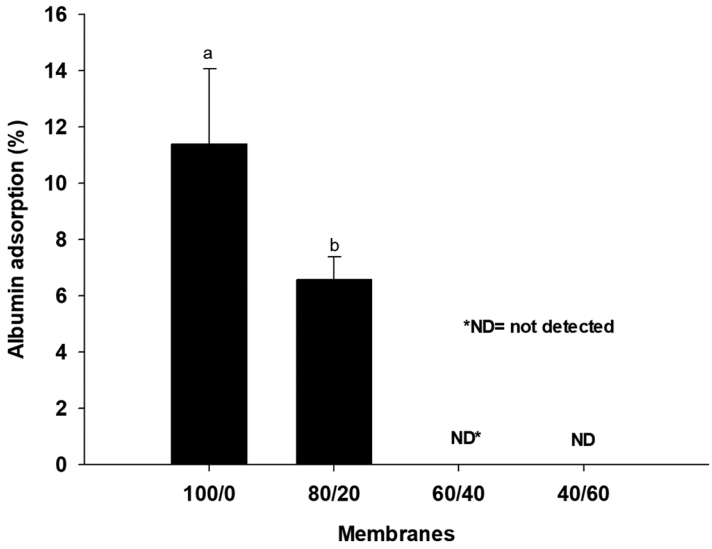

Figure 7: Adsorption (%) of human serum albumin of the PC/CM membranes

3.7 Erythrocyte Biocompatibility

The 40/60 membrane showed good biocompatibility with the erythrocytes (2.94%). Increased hemolysis percentage was a response to increased PC in the membrane composition; 60/40 (56.9%), 80/20 (65.6%), and control (75.6%) (Fig. 8). The high hemolysis percentage shown by the PC has not been reported previously, although it has been considered a biopolymer with low hemolytic capacity (less than 5%) [59–61]. We consider that high hemolysis showed by PC, probably is related to the type of PC used (food grade) in our study, which contained a high content of glucose proportions PC = 113 mg/dL; 80/20 = 106 mg/dL; 60/40 = 65 mg/dL; 40/60 mg/dL which was measured by the oxidase/peroxidase method. A high concentration of extracellular glucose likely causes changes in the osmotic pressure by modifying both $[Na^+]$ and $[K^+]$ intracellular. Protein glycation may also induce irreversible changes in the erythrocyte membrane [61]. The ≈5% hemolysis has been considered acceptable for biomaterials [62], indicating that the 40/60 membrane has good biocompatibility, influenced mainly by the CM.

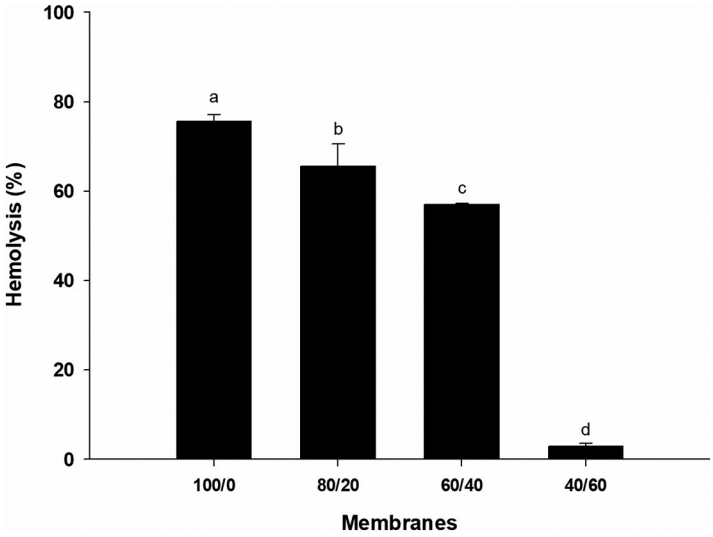

Figure 8: Percentage of hemolysis of erythrocytes incubated with PC/CM membranes

4 Conclusion

Blending CM with PC matrix can be used to develop membranes with novel properties. These blends resulted in thinner, transparent, yellow color, and low UV blocking capacity membranes. The microstructure of the PC membrane showed channels that vanished with the CM addition, but the new formation of microcapsules appeared in different shapes (sphere and ovoid). FTIR analysis suggested an intermolecular interaction between PC-PC, PC-CM, and CM-CM blends that may induce a molecular reorganization for the encapsulation of CM inside the membranes. On the other hand, the incorporation of CM increased the toughness, flexibility, and thermal stability of the membranes. The biological tests indicated a <5% of hemolysis for the 40/60 membrane, although, limited serum albumin adsorption. The PC/CM membrane is a potential biomaterial to develop different tools for human health.

Funding Statement: The authors acknowledge the support of the Division of Biological Science and Health of the University of Sonora for the Project USO313006744.

Conflicts of Interest: The authors declare that they have no conflicts of interest to report regarding the present study.

References

1. Sionkowska, A. (2011). Current research on the blends of natural and synthetic polymers as new biomaterials: Review. *Progress in Polymer Science, 36(9),* 1254–1276. https://doi.org/10.1016/j.progpolymsci.2011.05.003
2. Park, S. B., Lih, E., Park, K. S., Joung, Y. K., Han, D. K. (2017). Biopolymer-based functional composites for medical applications. *Progress in Polymer Science, 68(103A),* 77–105. https://doi.org/10.1016/j.progpolymsci.2016.12.003
3. Sohn, Y. J., Kim, H. T., Baritugo, K. A., Jo, S. Y., Song, H. M. et al. (2020). Recent advances in sustainable plastic upcycling and biopolymers. *Biotechnology Journal, 15(6),* 1900489. https://doi.org/10.1002/biot.201900489
4. de Campo, C., dos Santos, P. P., Costa, T. M. H., Paese, K., Guterres, S. S. et al. (2017). Nanoencapsulation of chia seed oil with chia mucilage (*Salvia hispanica* L.) as wall material: Characterization and stability evaluation. *Food Chemistry, 234(1),* 1–9. https://doi.org/10.1016/j.foodchem.2017.04.153

5. Morales, A., Labidi, J., Gullón, P., Astray, G. (2021). Synthesis of advanced biobased green materials from renewable biopolymers. *Current Opinion in Green and Sustainable Chemistry, 29,* 100436. https://doi.org/10.1016/j.cogsc.2020.100436
6. Ali Akbari Ghavimi, S., Ebrahimzadeh, M. H., Solati-Hashjin, M., Abu Osman, N. A. (2015). Polycaprolactone/starch composite: Fabrication, structure, properties, and applications. *Journal of Biomedical Materials Research Part A, 103(7),* 2482–2498. https://doi.org/10.1002/jbm.a.35371
7. Cherian, B. M., Leão, A. L., de Souza, S. F., Costa, L. M. M., de Olyveira, G. M. et al. (2011). Cellulose nanocomposites with nanofibres isolated from pineapple leaf fibers for medical applications. *Carbohydrate Polymers, 86(4),* 1790–1798. https://doi.org/10.1016/j.carbpol.2011.07.009
8. Kamel, R., Afifi, S. M., Kassem, I. A., Elkasabgy, N. A., Farag, M. A. (2020). Arabinoxylan and rhamnogalacturonan mucilage: Outgoing and potential trends of pharmaceutical, environmental, and medicinal merits. *International Journal of Biological Macromolecules, 165(6),* 2550–2564. https://doi.org/10.1016/j.ijbiomac.2020.10.175
9. Eivazzadeh-Keihan, R., Noruzi, E. B., Aliabadi, H. A. M., Sheikhaleslami, S., Akbarzadeh, A. R. et al. (2022). Recent advances on biomedical applications of pectin-containing biomaterials. *International Journal of Biological Macromolecules, 217,* 1–18. https://doi.org/10.1016/j.ijbiomac.2022.07.016
10. Mendes, J. P., Esperança, J., Medeiros, M. J., Pawlicka, A., Silva, M. M. (2017). Structural, morphological, ionic conductivity, and thermal properties of pectin-based polymer electrolytes. *Molecular Crystals and Liquid Crystals, 643(1),* 266–273. https://doi.org/10.1080/15421406.2016.1263111
11. Li, C., Nie, H., Chen, Y., Xiang, Z. Y., Li, J. B. (2016). Amide pectin: A carrier material for colon-targeted controlled drug release. *Journal of Applied Polymer Science, 133(29),* 43697. https://doi.org/10.1002/app.43697
12. Gomez-Rodriguez, G. H., Lopez-Mata, M. A., Valbuena-Gregorio, E., Melchor, R. G. V., Campos-Garcia, J. C. (2018). Microencapsulation of carvacrol using pectin/aloe-gel as a novel wound dressing films. *Current Topics in Medicinal Chemistry, 18(14),* 1261–1268. https://doi.org/10.2174/1568026618666180810141455
13. Noh, J., Kim, J., Kim, J. S., Chung, Y. S., Chang, S. T. et al. (2018). Microencapsulation by pectin for multi-components carriers bearing both hydrophobic and hydrophilic active agents. *Carbohydrate Polymers, 182(5330),* 172–179. https://doi.org/10.1016/j.carbpol.2017.11.026
14. Belščak-Cvitanović, A., Bušić, A., Barišić, L., Vrsaljko, D., Karlović, S. (2016). Emulsion templated microencapsulation of dandelion (*Taraxacum officinale* L.) polyphenols and β-carotene by ionotropic gelation of alginate and pectin. *Food Hydrocolloids, 57(3),* 139–152. https://doi.org/10.1016/j.foodhyd.2016.01.020
15. Knez Hrnčič, M., Ivanovski, M., Cör, D., Knez, Ž. (2019). Chia seeds (*Salvia hispanica* L.): An overview—phytochemical profile, isolation methods, and application. *Molecules, 25(1),* 11. https://doi.org/10.3390/molecules25010011
16. Dick, M., Costa, T. M. H., Gomaa, A., Subirade, M., de Oliveira Rios, A., et al. (2015). Edible film production from chia seed mucilage: Effect of glycerol concentration on its physicochemical and mechanical properties. *Carbohydrate Polymers, 130(8),* 198–205. https://doi.org/10.1016/j.carbpol.2015.05.040
17. Cortés-Camargo, S., Acuña-Avila, P. E., Rodríguez-Huezo, M. E., Román-Guerrero, A., Varela-Guerrero (2019). Effect of chia mucilage addition on oxidation and release kinetics of lemon essential oil microencapsulated using mesquite gum-Chia mucilage mixtures. *Food Research International, 116(8),* 1010–1019. https://doi.org/10.1016/j.foodres.2018.09.040
18. Lin, K. Y., Daniel, J. R., Whistler, R. L. (1994). Structure of chia seed polysaccharide exudate. *Carbohydrate Polymers, 23(1),* 13–18. https://doi.org/10.1016/0144-8617(94)90085-X
19. Velázquez-Gutiérrez, S. K., Figueira, A. C., Rodríguez-Huezo, M. E., Román-Guerrero, A., Carrillo-Navas et al. (2015). Sorption isotherms, thermodynamic properties and glass transition temperature of mucilage extracted from chia seeds (*Salvia hispanica* L.). *Carbohydrate Polymers, 121(6),* 411–419. https://doi.org/10.1016/j.carbpol.2014.11.068
20. da Silveira Ramos, I. F., Magalhães, L. M., do O Pessoa, C., Ferreira, P. M. P., dos Santos Rizzo, M. et al. (2021). New properties of chia seed mucilage (*Salvia hispanica* L.) and potential application in cosmetic and

pharmaceutical products. *Industrial Crops and Products, 171(1),* 113981. https://doi.org/10.1016/j.indcrop.2021.113981

21. Mujtaba, M., Koc, B., Salaberria, A. M., Ilk, S., Cansaran-Duman, D. et al. (2019). Production of novel chia-mucilage nanocomposite films with starch nanocrystals; An inclusive biological and physicochemical perspective. *International Journal of Biological Macromolecules, 133,* 663–673. https://doi.org/10.1016/j.ijbiomac.2019.04.146
22. Muñoz, L. A., Aguilera, J. M., Rodriguez-Turienzo, L., Cobos, A., Diaz, O. (2012). Characterization and microstructure of films made from mucilage of *Salvia hispanica* and whey protein concentrate. *Journal of Food Engineering, 111(3),* 511–518. https://doi.org/10.1016/j.jfoodeng.2012.02.031
23. Mujtaba, M., Akyuz, L., Koc, B., Kaya, M., Ilk, S. et al. (2019). Novel, multifunctional mucilage composite films incorporated with cellulose nanofibers. *Food Hydrocolloids, 89(7),* 20–28. https://doi.org/10.1016/j.foodhyd.2018.10.021
24. Dehghani, S., Noshad, M., Rastegarzadeh, S., Hojjati, M., Fazlara, A. (2020). Electrospun chia seed mucilage/PVA encapsulated with green cardamonmum essential oils: Antioxidant and antibacterial property. *International Journal of Biological Macromolecules, 161(8),* 1–9. https://doi.org/10.1016/j.ijbiomac.2020.06.023
25. Luo, M., Cao, Y., Wang, W., Chen, X., Cai, J. et al. (2019). Sustained-release antimicrobial gelatin film: Effect of chia mucilage on physicochemical and antimicrobial properties. *Food Hydrocolloids, 87(5),* 783–791. https://doi.org/10.1016/j.foodhyd.2018.09.010
26. Ağçeli, G. K. (2022). A new approach to nanocomposite carbohydrate polymer films: Levan and chia seed mucilage. *International Journal of Biological Macromolecules, 218(4),* 751–759. https://doi.org/10.1016/j.ijbiomac.2022.07.157
27. Kučka, M., Ražná, K., Harenčár, Ľ., Kolarovičová, T. (2022). Plant seed mucilage—Great potential for sticky matter. *Nutraceuticals, 2(4),* 253–269. https://doi.org/10.3390/nutraceuticals2040019
28. Han, J. H., Floros, J. D. (1997). Casting antimicrobial packaging films and measuring their physical properties and antimicrobial activity. *Journal of Plastic Film & Sheeting, 13(4),* 287–298. https://doi.org/10.1177/875608799701300405
29. Carneiro-da-Cunha, M. G., Cerqueira, M. A., Souza, B. W. S., Souza, M. P., Teixeira, J. A. et al. (2009). Physical properties of edible coatings and films made with a polysaccharide from *Anacardium occidentale* L. *Journal of Food Engineering, 95(3),* 379–385. https://doi.org/10.1016/j.jfoodeng.2009.05.020
30. Reed, S. J. B. (2005). *Electron microprobe analysis and scanning electron microscopy in geology.* USA: Cambridge University Press.
31. Su, J. F., Yuan, X. Y., Huang, Z., Wang, X. Y., Lu, X. Z. et al. (2012). Physicochemical properties of soy protein isolate/carboxymethyl cellulose blend films crosslinked by Maillard reactions: Color, transparency and heat-sealing ability. *Materials Science and Engineering: C, 32(1),* 40–46. https://doi.org/10.1016/j.msec.2011.09.009
32. Wang, Y., Wang, C., Xie, Y., Yang, Y., Zheng, Y. (2019). Highly transparent, highly flexible composite membrane with multiple antimicrobial effects used for promoting wound healing. *Carbohydrate Polymers, 222(6),* 114985. https://doi.org/10.1016/j.carbpol.2019.114985
33. Cazón, P., Vázquez, M., Velazquez, G. (2018). Cellulose-glycerol-polyvinyl alcohol composite films for food packaging: Evaluation of water adsorption, mechanical properties, light-barrier properties and transparency. *Carbohydrate Polymers, 195(21),* 432–443. https://doi.org/10.1016/j.carbpol.2018.04.120
34. Rao, M. S., Kanatt, S. R., Chawla, S. P., Sharma, A. (2010). Chitosan and guar gum composite films: Preparation, physical, mechanical and antimicrobial properties. *Carbohydrate Polymers, 82(4),* 1243–1247. https://doi.org/10.1016/j.carbpol.2010.06.058
35. López-Mata, M. A., García-González, G., Valbuena-Gregorio, E., Ruiz-Cruz, S., Zamudio-Flores, P. B. et al. (2016). Development and characteristics of biodegradable Aloe-gel/egg white films. *Journal of Applied Polymer Science, 133(40),* R30. https://doi.org/10.1002/app.44067
36. da Silva Oliveira, C. I., Martinez-Martinez, D., Al-Rjoub, A., Rebouta, L., Menezes, R. et al. (2018). Development of a statistical method to help evaluating the transparency/opacity of decorative thin films. *Applied Surface Science, 438,* 51–58. https://doi.org/10.1016/j.apsusc.2017.10.017

37. de Souza Coelho, C. C., Silva, R. B. S., Carvalho, C. W. P., Rossi, A. L., Teixeira, J. A. et al. (2020). Cellulose nanocrystals from grape pomace and their use for the development of starch-based nanocomposite films. *International Journal of Biological Macromolecules, 159,* 1048–1061. https://doi.org/10.1016/j.ijbiomac.2020.05.046
38. López-Mata, M. A., Gastelum-Cabrera, M., Valbuena-Gregorio, E., Zamudio-Flores, P. B., Burruel-Ibarra et al. (2018). Physicochemical properties of novel pectin/Aloe gel membranes. *Iranian Polymer Journal, 27(8),* 1–9. https://doi.org/10.1007/s13726-018-0631-8
39. Ibuki, Y., Komaki, Y., Yang, G., Toyooka, T. (2021). Long-wavelength UVA enhances UVB-induced cell death in cultured keratinocytes: DSB formation and suppressed survival pathway. *Photochemical & Photobiological Sciences, 20(5),* 639–652. https://doi.org/10.1007/s43630-021-00050-w
40. Lee, R., Pranata, M., Ustunol, Z., Almenar, E. (2013). Influence of glycerol and water activity on the properties of compressed egg white-based bioplastics. *Journal of Food Engineering, 118(1),* 132–140. https://doi.org/10.1016/j.jfoodeng.2013.03.031
41. Cokaygil, Z., Banar, M., Seyhan, A. T. (2014). Orange peel-derived pectin jelly and corn starch-based biocomposite film with layered silicates. *Journal of Applied Polymer Science, 131(16),* 40654. https://doi.org/10.1002/app.40654
42. Krystyjan, M., Khachatryan, G., Ciesielski, W., Buksa, K., Sikora, M. (2017). Preparation and characteristics of mechanical and functional properties of starch/*Plantago psyllium* seeds mucilage films. *Starch-Stärke, 69(11–12),* 1700014. https://doi.org/10.1002/star.201700014
43. Bermúdez-Oria, A., Rodríguez-Gutiérrez, G., Vioque, B., Rubio-Senent, F., Fernández-Bolaños, J. (2017). Physical and functional properties of pectin-fish gelatin films containing the olive phenols hydroxytyrosol and 3,4-dihydroxyphenylglycol. *Carbohydrate Polymers, 178,* 368–377. https://doi.org/10.1016/j.carbpol.2017.09.042
44. Chambi, H. N. M., Grosso, C. R. F. (2011). Mechanical and water vapor permeability properties of biodegradables films based on methylcellulose, glucomannan, pectin and gelatin. *Food Science and Technology, 31(3),* 739–746. https://doi.org/10.1590/S0101-20612011000300029
45. Younis, H. G., Zhao, G. (2019). Physicochemical properties of the edible films from the blends of high methoxyl apple pectin and chitosan. *International Journal of Biological Macromolecules, 131(2),* 1057–1066. https://doi.org/10.1016/j.ijbiomac.2019.03.096
46. Pasini Cabello, S. D., Takara, E. A., Marchese, J., Ochoa, N. A. (2015). Influence of plasticizers in pectin films: Microstructural changes. *Materials Chemistry and Physics, 162(Supplement C),* 491–497. https://doi.org/10.1016/j.matchemphys.2015.06.019
47. Chin, S. S., Lyn, F. H., Hanani, Z. N. (2017). Effect of Aloe vera (*Aloe barbadensis* Miller) gel on the physical and functional properties of fish gelatin films as active packaging. *Food Packaging and Shelf Life, 12(1),* 128–134. https://doi.org/10.1016/j.fpsl.2017.04.008
48. Luo, M., Cao, Y., Wang, W., Chen, X., Cai, J. et al. (2019). Sustained-release antimicrobial gelatin film: Effect of chia mucilage on physicochemical and antimicrobial properties. *Food Hydrocolloids, 87(5),* 783–791. https://doi.org/10.1016/j.foodhyd.2018.09.010
49. Espitia, P. J. P., Du, W. X., de Jesús Avena-Bustillos, R., de Soares, N. F. F., McHugh, T. H. (2014). Edible films from pectin: Physical-mechanical and antimicrobial properties—A review. *Food Hydrocolloids, 35(6),* 287–296. https://doi.org/10.1016/j.foodhyd.2013.06.005
50. Giancone, T., Torrieri, E., Di Pierro, P., Cavella, S., Giosafatto, C. V. L. et al. (2011). Effect of surface density on the engineering properties of high methoxyl pectin-based edible films. *Food and Bioprocess Technology, 4(7),* 1228–1236. https://doi.org/10.1007/s11947-009-0208-9
51. Mu, C., Guo, J., Li, X., Lin, W., Li, D. (2012). Preparation and properties of dialdehyde carboxymethyl cellulose crosslinked gelatin edible films. *Food Hydrocolloids, 27(1),* 22–29. https://doi.org/10.1016/j.foodhyd.2011.09.005
52. Wilson, C. J., Clegg, R. E., Leavesley, D. I., Pearcy, M. J. (2005). Mediation of biomaterial-cell interactions by adsorbed proteins: A review. *Tissue Engineering, 11(1–2),* 1–18. https://doi.org/10.1089/ten.2005.11.1

53. Cacicedo, M. L., Islan, G. A., Drachemberg, M. F., Alvarez, V. A., Bartel, L. C. et al. (2018). Hybrid bacterial cellulose-pectin films for delivery of bioactive molecules. *New Journal of Chemistry, 42(9),* 7457–7467. https://doi.org/10.1039/C7NJ03973E
54. Wang, R., Liang, R., Dai, T., Chen, J., Shuai, X. et al. (2019). Pectin-based adsorbents for heavy metal ions: A review. *Trends in Food Science & Technology, 91(3),* 319–329. https://doi.org/10.1016/j.tifs.2019.07.033
55. Popov, S., Paderin, N., Khramova, D., Kvashninova, E., Melekhin, A. et al. (2022). Characterization and biocompatibility properties *in vitro* of gel beads based on the pectin and κ-carrageenan. *Marine Drugs, 20(2),* 94. https://doi.org/10.3390/md20020094
56. Visalakshan, R. M., MacGregor, M. N., Sasidharan, S., Ghazaryan, A., Mierczynska-Vasilev, A. M. et al. (2019). Biomaterial surface hydrophobicity-mediated serum protein adsorption and immune responses. *ACS Applied Materials & Interfaces, 11(31),* 27615–27623. https://doi.org/10.1021/acsami.9b09900
57. Tao, C., Zhu, W., Iqbal, J., Xu, C., Wang, D. A. (2020). Stabilized albumin coatings on engineered xenografts for attenuation of acute immune and inflammatory responses. *Journal of Materials Chemistry B, 8(28),* 6080–6091. https://doi.org/10.1039/D0TB01111H
58. Dabare, R. L., Bachhuka, P., Palms, A., Parkinson-Lawrence, D., Hayball, E. et al. (2022). Surface chemistry mediated albumin adsorption, conformational changes and influence on innate immune responses. *Applied Surface Science, 596(3),* 153518. https://doi.org/10.1016/j.apsusc.2022.153518
59. Konovalova, M. V., Markov, P. A., Durnev, E. A., Kurek, D. V., Popov, S. V. et al. (2017). Preparation and biocompatibility evaluation of pectin and chitosan cryogels for biomedical application. *Journal of Biomedical Materials Research Part A, 105(2),* 547–556. https://doi.org/10.1002/jbm.a.35936
60. Şahin, G., Sanajou, S., Behnoush, R., Bahramzade, E. (2019). Adsorption of iron, lead, paracetamol, imipramine on natural polymers. *EMU Journal of Pharmaceutical Sciences, 2(1),* 33–54.
61. Anandan, S., Mahadevamurthy, M., Ansari, M. A., Alzohairy, M. A., Alomary, M. N. et al. (2019). Biosynthesized ZnO-NPs from Morus indica attenuates methylglyoxal-induced protein glycation and RBC damage: *In-vitro, in-vivo* and molecular docking study. *Biomolecules, 9(12),* 882. https://doi.org/10.3390/biom9120882
62. Hira, I., Kumar, R., Saini, A. K., Gullilat, H., Saini, V. et al. (2022). Apoptotic cell death induction through pectin, guar gum and zinc oxide nanocomposite in A549 lung adenocarcinomas. *Biointerface Research in Applied Chemistry, 12(2),* 1856–1869. https://doi.org/10.33263/BRIAC122.18561869